DAMAGE AND PERMEABILITY OF COMPOSITE LAMINATES

Hortense Laeuffer[1,2], Christophe Bois[2], Jean-Christophe Wahl[2], Nicolas Perry[3], and Florian Lavelle[1]

[1]Direction des LAnceurs (DLA), CNES
52, rue Jacques Hillairet, 75612 PARIS Cedex, France
Email : h.laeuffer@i2m.u-bordeaux1.fr

[2]Univ. Bordeaux, I2M, UMR 5295, F-33400 Talence, France.
IUT, 15 rue Naudet, 33175 Gradignan, France
Email : c.bois@i2m.u-bordeaux1.fr
Email : jc.wahl@i2m.u-bordeaux1.fr

[3]Arts et Metiers ParisTech, I2M, UMR 5295, F-33400 Talence, France.
Esplanade des Arts et Métiers, 33405 Talence Cedex, France
Email : n.perry@i2m.u-bordeaux1.fr

Keywords: damage, transverse crack, permeability, leak path, polymer-matrix composite, storage vessel

ABSTRACT

This study focuses on the link between damage development and permeability evolution of composite laminates. By making use of an original device, measurement of the permeability of composite pipes under pressure and quantification of leak paths were conducted. Presented results show that very few (about one per 100 cm²) leak paths are sufficient to increase the permeability of several orders of magnitude, suggesting the existence of a preliminary phase characterized by a progressive development of a few cracks. Damage modelling and identification are proposed, allowing this phase to be taken into account. From this modelling coupled with a simplified representation of the crack network, prediction of leak path density is provided.

1 INTRODUCTION

Lightening the structure of launcher vehicles increases their cost-efficiency, which is a core issue for space industry. This leads to an extensive use of composite materials for space applications. In the case of propellant tanks, removing the impermeable liner allows reducing the weight, and thereby increasing the payload, while reducing the manufacturing costs. As a counterpart, the gas barrier function of the tank only relies on the composite laminate it-self.

Due to the heterogeneous nature of polymer-matrix composites, transverse cracking and micro-delamination may occur for low thermo-mechanical loading cases, with very little effect on the stiffness and strength. Micro-delamination allows cracks of adjacent plies to connect together into a crack network, as shown in Fig.1. When all the plies are damaged, the network goes through the whole thickness of the tank, resulting in leakage path creation.

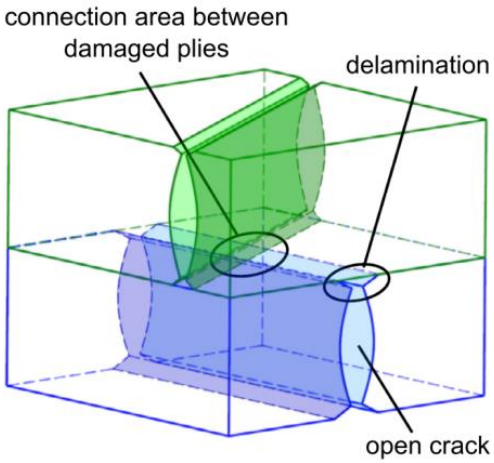

Figure 1: Crack network in two damaged plies, after [1].

Therefore, linerless-composite pressure vessels have to be designed with respect to the two functions of the composite wall: permeability and mechanical strength. This study addresses part of experimental observations and resulting reflexion on the development of prediction models of the link between damage development and permeability evolution of composite laminates.

2 MEASUREMENT OF PERMEABILITY EVOLUTION WITH DAMAGE DEVELOPMENT

2.1 General framework

Permeability is the ability of a material to transmit fluids when submitted to a pressure gradient. It has been defined by Darcy [2] as the proportionality link between the gas flow rate, the physical properties of the gas and the pressure gradient applied to a specimen:

$$q = \frac{Q}{S} = \frac{k}{\mu}\frac{dp}{dx} \tag{1}$$

for a Newtonian fluid, with:

k: material permeability (m^2);
S: measurement area (m^2);
Q: leakage rate (m^3/s);
μ: dynamic viscosity of gas (Pa.s);
$\frac{dp}{dx}$: pressure gradient through the thickness (Pa/m).

A generic permeability determination method consists in keeping constant two of the following quantities: upstream and downstream pressure and leakage rate, while measuring variations of the third. Because composite are very weakly permeable ($k \cong 10^{-23}$ for an undamaged laminate [3]), accurately measuring Q would be practically impossible. Therefore, the usual measure is a pressure loss or gain.

2.2 Permeability and leak path: measurement process

The experimental device consists in a composite pipe closed by two thrust plates, as shown in Fig.2. Polymer rings and sealing joints prevent leakage between the end of the pipe and the plates. It allows pressuring the pipe and measuring the pressure decay over time. Assuming the atmospheric pressure is constant and the flow is quasi-steady, the outgoing flow rate is considered as constant provided the pressure decay is not too important (*i.e.* a few percent of initial internal pressure). The

measurement method is similar to that introduced in Ref. [3].

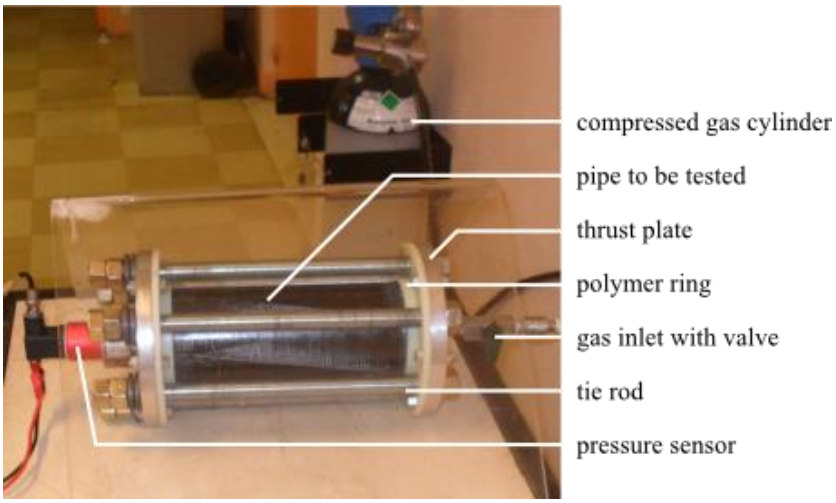

Figure 2: Experimental device for pressurization and permeability measurement of pipes.

The internal pressure of the pipe is set with compressed gas. Then, the valve of the device is closed and the measurement of the internal pressure is launched. While the pressure decay is being measured, it is possible to count and localize leak paths over the external area of the pipe by making use of leak detector spay. At the end of the measurement step (which has to be long enough to detect a pressure decay in the pipe), the measurement data are processed in order to extract the pressure decay over time and the average pressure. Assuming that the gas is ideal and its compressibility has little effect, and that deformations of the porous medium are negligible, the permeability can finally be written as follows:

$$k = \frac{2\mu LV}{S\left(p_{ext}^2 - p_{int}^2\right)} \frac{dp_{int}}{dt} \tag{2}$$

where L stands for the thickness, V for the internal gas volume, S for the external pipe area, p_{ext} and p_{int} for external and internal pressure, and dp_{int}/dt for the variation of the internal pressure over time.

After each measurement step, the device can be set to a lower pressure, in order to examine the effect of the crack closure on the permeability or to a larger pressure in order to allow damage development and creation of new leakage paths.

2.3 Experimental settings

The tested specimen is a filament-wound pipe of 100mm diameter and 200 mm length. The material is T700 carbon fibre and epoxy matrix and the stratification is [+45/-45/+45/-45]. Permeant gas is nitrogen.

Several permeability measurements have been done for four different damage states. That is to say, for each damage state the pressure has been set to a maximal pressure, allowing damage to develop and leak path to appear in the pipe, at the same time leak paths were localized and counted, thereafter multiple permeability measurement has been run, decreasing the pressure step by step while no crack could develop.

2.4 Results and analysis

Results are shown in Fig.3. Complete testing of the pipe took a month and a half. Initial permeability is lower than 10^{-22} m^2. The permeability drop at the beginning of the test might be a

reduction of intrinsic leakage of the device, due to pressure pushing pipe ends on sealing joints. Permeability increase before first leak path occurs may be due to cracking of external plies only, lower scale damage, device leakage or undetected leak paths. Such a tiny permeability is tricky to measure and not significant for the present study.

For each new loading step, *i.e.* when pressure is set to a new maximal value, the permeability increases of almost one order of magnitude while the number of leak path evolves slowly: from 1 to 12 for permeability values from 7.10^{-21} m^2 (first leak path) to 8.10^{-19} m^2. Each new damage state is followed by several permeability measurements for lower pressure values, for which permeability decreases slowly with the mechanical loading but never reach the initial permeability. This correlates with a partial closure of cracks due to residual stresses of thermo-mechanical origin. These facts lead to the conclusion that a few leak paths generate a large variation of permeability.

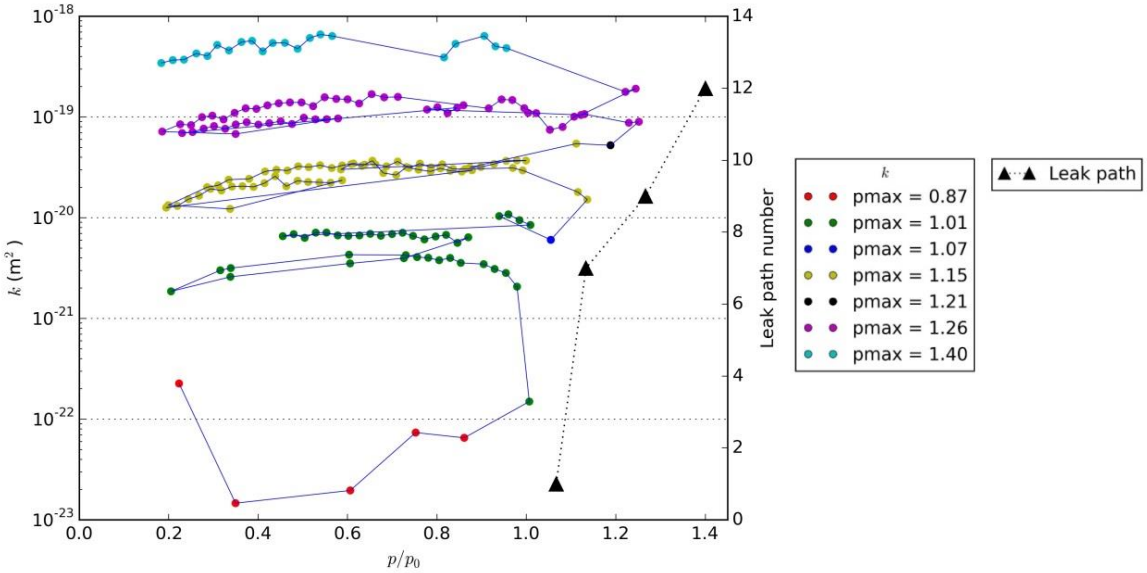

Figure 3: Permeability and leak paths measurement vs. internal pressure on a pipe of 100 mm diameter, 200 mm length and [+45/-45/+45/-45] lay-up
(pressure adimensioned with respect to first-leak-path pressure).

Permeability of composite laminates seems to be very sensitive to the first phase of damage development. For this reason, this part of the damage scenario is investigated in next section.

3 DAMAGE DESCRIPTION AND MODELLING

3.1 Damage measurement and description

Damage measurement is done on tensile test specimens, of which one edge has been polished over the full length. An optical microscope with vertical travelling device allows observing damage development in transverse plies, while the specimen undergoes several loading steps, as shown in Fig.4(a).

One damage state is defined by its crack rate ρ and delamination length at crack tips μ, as illustrated in Fig.4(b). The crack rate ρ is the average number of cracks over the observed length L. This damage representation is convenient because of its physical nature and direct link with leakage path creation.

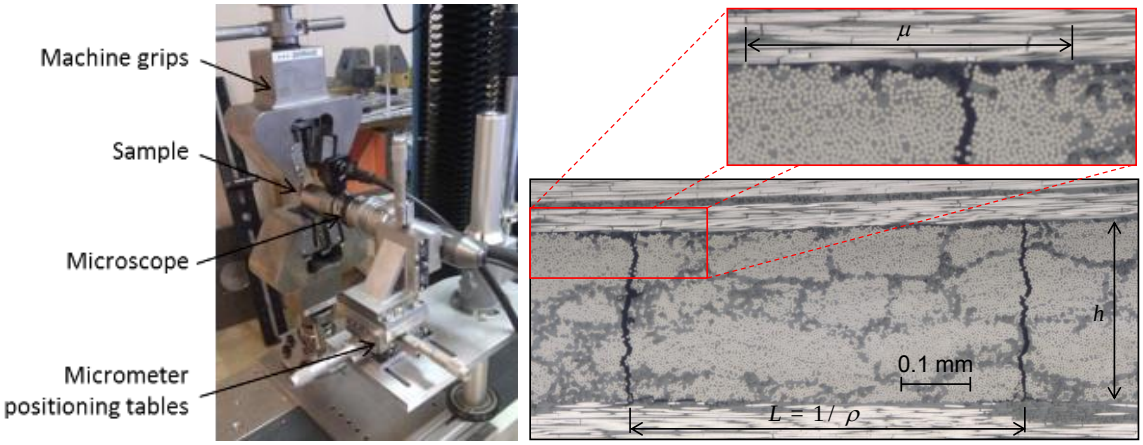

Figure 4: Damage observation under tensile loading test (a) and micrograph of the edge of the specimen: illustration of transverse cracks and short delamination at crack tip (b), after [3].

3.2 Damage model description

The damage model aims to predict development of transverse cracks associated to short delamination at crack tip according to load history. The study focuses on unidirectional ply loaded with in-plane stresses.

The damage model used here is fully described in Ref. [1]. It is based on the multi-scale damage model proposed by Huchette from ONERA research team [4,5]. It has the advantage that the damage state is represented by two physical variables, crack density ρ and delamination length μ previously defined in Fig.2. Experimentally, the distance between two transverse cracks and delamination length at crack tips are subjected to variations. In the model, ρ and μ are thus defined as representative variables of a locally periodic pattern [6]. In order to simplify and generalise damage effect on stiffness and damage evolution laws, adimensional damage variables are defined as follows:

$$\bar{\rho} = \rho h \tag{3}$$

$$\bar{\mu} = \mu \rho \tag{4}$$

where h is the thickness of the composite ply being considered.

On the same scheme, the crack opening displacement can be computed from any set of damage variables $\bar{\rho}$ and $\bar{\mu}$ [1].

3.3 Damage development characteristics

Model identification relies on damage measurement previously described. It consists in determining the initiation thresholds and evolution laws of the material damage from the experimental data.

As demonstrated by several authors, an energy criterion is necessary to predict crack growth and take into account the effect of ply thickness on the initiation threshold of transverse cracks [7–9], while, a stress criterion is also required to represent crack onset (due to local degradation). In fact, transverse crack development requires that energy and stress criteria are simultaneously verified. Since energy release rate (energy per unit of cracked area) is directly proportional to ply thickness, while stress and strain are not dependent to ply thickness, the critical criterion will be the energy criterion for thin ply and stress criterion for thick ply. Typically, for the prepreg unidirectional carbon fibre composite T700GC/M21 used in this study, the transition between the two criteria is reached for a thickness close to 0.72 mm. Note that under this value, the initiation threshold is inversely proportional to ply thickness which makes thin plies very competitive for permeability requirements.

The identification of these criteria, obviously, requires testing at least 2 laminates with different ply thicknesses.

Damage variables are driven by evolution laws build on experimental observations:

$$\bar{\rho} = \sup_{\tau \le t} \left(\frac{K_1}{1 + \frac{K_2}{h}\bar{\mu}} \left(\gamma_{\bar{\rho}} \langle \sqrt{y_{\bar{\rho}_I}} - \sqrt{{y^s}_{\bar{\rho}_I}} \rangle + (1 - \gamma_{\bar{\rho}}) \langle \sqrt{y_{\bar{\rho}_{II}}} - \sqrt{{y^s}_{\bar{\rho}_{II}}} \rangle \right) \right) \tag{5}$$

$$\bar{\mu} = 1 - \exp\left(-\bar{\rho} \frac{\gamma_{\bar{\mu}} y_{\bar{\mu}_I} + (1 - \gamma_{\bar{\mu}}) y_{\bar{\mu}_{II}}}{K_3} \right) \tag{6}$$

where K_1 and K_3 are the damage evolution speed, K_2 the slowing of transverse cracking due to delamination, $\gamma_{\bar{\rho}}$ and $\gamma_{\bar{\mu}}$ the mode I / mode II ratio, $y_{\bar{\rho}_I}, y_{\bar{\rho}_{II}}, y_{\bar{\mu}_I}, y_{\bar{\mu}_{II}}$ the thermodynamical forces for each rupture mode (opening and plane shear) associated to each damage variable, ${y^s}_{\bar{\rho}_I}$ and ${y^s}_{\bar{\rho}_{II}}$ the damage thresholds. These evolution laws ensure that delamination can't occur before transverse cracking, and that transverse cracks are more difficult to create in a strongly delaminated structure.

For a standard design, normally consisting of a prediction of damage densities and induced stiffness losses, early cracks are not relevant because of their little effect on mechanical properties. Therefore, usual damage models only predict the fast evolution of the damage state since the initiation threshold is reached. For this reason, damage evolution laws are not progressive and model characteristics are identified by observation of damage development over a length of at most L=20 mm. The minimal available crack rate will therefore depend on the length of the observed area, and the initiation threshold might be overestimated. The slow evolution of the leak-path number shown in Fig.3 suggests the existence of a preliminary phase characterized by a progressive development of a few cracks, due to the presence of defects (voids, high-matrix areas, ply waviness…). We thus propose to identify damage development by observing a larger area.

3.4 Damage measure: conducted experiments

Following experimental results come from damage observation over 92 mm length of the edge of a tensile test specimen. Material is prepreg unidirectional carbon fibre composite T700GC/M21, ply thickness is 0.26 mm and stratification is [0/0/90/90/90/0/0]. Order of creation, crack position and associated loading were recorded. Delamination length and crack opening were also examined but are not used here.

3.5 Results and analysis

Fig.5 shows position of existent cracks for five loading steps. We observe a scattering of the average distance between two adjacent cracks. Therefore, crack rate and initiation threshold will obviously depend on the length and position of the observation area. Fig.6(a) is the evolution of the crack rate with respect to the loading, computed on the whole length. It shows the existence of a first phase in damage development during which crack rate increases slowly. With a smaller observation length, the sampling is smaller and does not permit a representative observation of this phase. Crack rate $\bar{\rho}$ has been processed over smaller observation areas so as to determine the average stress of first crack creation with respect to the length of the area L_{obs}. Fig.6(b) highlights the existence of a characteristic length of about 40 mm below which the initiation threshold is overestimated. Experiments on a larger batch of specimens, possibly with larger observation length, have to be carried in order to confirm this trend. Test on others stratifications are also needed to characterize ply thickness effect and properties in mode II (plane shear).

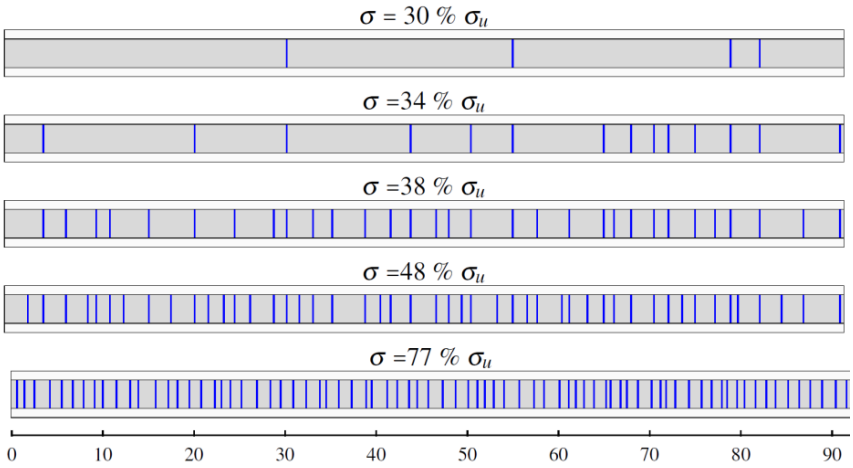

Figure 5: Schematic representation of cracks over 92 mm of the observed edge of a tensile test specimen for five loading steps.

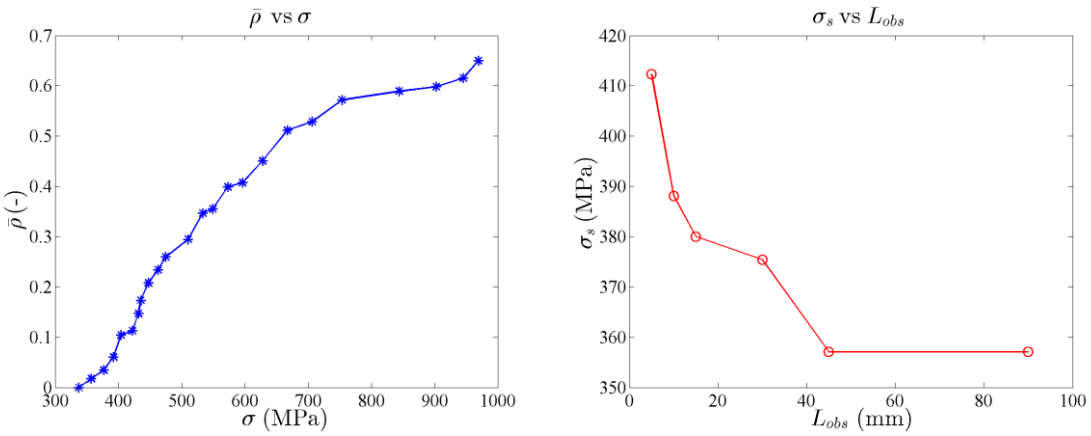

(a) (b)

Figure 6: Crack rate vs. stress (a) and average identified initiation threshold with respect to the observed length (b).

3.6 Damage model identification

In order to describe the experimental evolution of $\bar{\rho}$ and its low slope at the beginning, we propose to make use of an enhanced evolution law. This law is built from Eq. 5 by multiplication with a Weibull repartition function:

$$\bar{\rho} = \sup_{\tau \le t} \left(\frac{K_1}{1 + \frac{K_2}{h}\bar{\mu}} F\left(y_{\bar{\rho}_I}, y_{\bar{\rho}_{II}}\right) \right) \times \left(1 - \exp\left(- \frac{F\left(y_{\bar{\rho}_I}, y_{\bar{\rho}_{II}}\right)}{\lambda} \right)^2 \right) \tag{7}$$

$$\text{with } F\left(y_{\bar{\rho}_I}, y_{\bar{\rho}_{II}}\right) = \gamma_{\bar{\rho}} \left\langle \sqrt{y_{\bar{\rho}_I}} - \sqrt{y^s{}_{\bar{\rho}_I}} \right\rangle + \left(1 - \gamma_{\bar{\rho}}\right) \left\langle \sqrt{y_{\bar{\rho}_{II}}} - \sqrt{y^s{}_{\bar{\rho}_{II}}} \right\rangle \tag{8}$$

where λ is the scale parameter which controls the transition from the first phase to the other. Results of this modelling are shown in Fig.7.

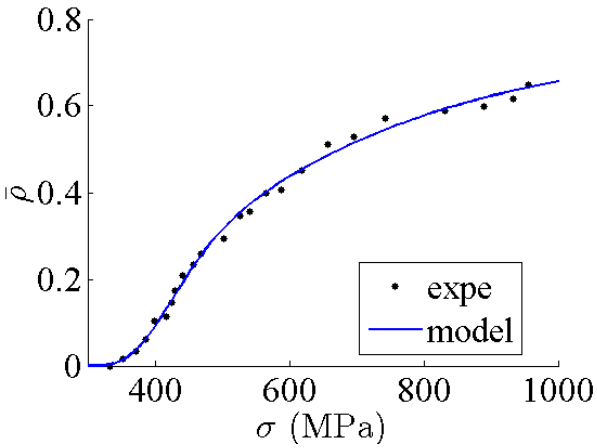

Figure 7: Crack density from experiment and simulation vs. stress.

4 STUDY OF THE LINK BETWEEN DAMAGE AND PERMEABILITY: LEAK PATH CREATION

4.1 Leak path density

As we can see on Fig.1 leak paths result from intersection of cracks of adjacent plies. In order to propose a simple evaluation of leak path number, several assumptions are made. Crack length is assumed to be infinite and crack intersection at an interface to be periodic. Size, and thus leakage rate of leak path is not addressed, delamination and crack opening insure connection but their magnitude is not taken into account. Leak path number is here defined as the minimal intersection number between cracks of adjacent plies. Hence, no leak path is created until at least one ply remains undamaged, and intersection number depends only on crack densities of adjacent plies ρ_i and ρ_{i+1}, and on the angle $(\theta_{i+1} - \theta_i)$, as illustrated in Fig.8.

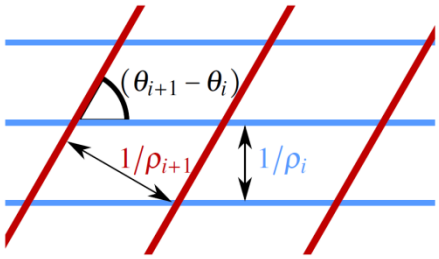

Figure 8: Schematic crack network.

Leak path density $\bar{\eta}$, leak path number N_{lp} and experimental $\bar{\eta}_{exp}$ are computed as follows:

$$\bar{\eta} = \min_{i=1,\dots,n-1} (\bar{\rho}_i \, \bar{\rho}_{i+1} \times |\sin(\theta_{i+1} - \theta_i)|) \tag{9}$$

$$N_{lp} = \min_{i=1,\dots,n-1} \left(\bar{\rho}_i \, \bar{\rho}_{i+1} \times \frac{|\sin(\theta_{i+1} - \theta_i)|}{h_i h_{i+1}} \right) \times S \tag{10}$$

$$\bar{\eta}_{exp} = \frac{h^2}{S} N_{pf\ exp} \tag{11}$$

with h_i the thickness of ply i, n the ply number of the laminate, and S the area of the tested zone (external area in the case of the pipe).

4.2 Application and results

Damage densities of the tested pipe have been simulated for conditions similar to those of the test using the progressive evolution law. Crack densities are used as input of the Eq. 9. Fig.9 shows that, despite of the progressivity added into the evolution law, the model predicts a fast increase of leak path number, which does not correlate with the observed evolution: leak path densities from the experiment are in between 6.10^{-7} and 7.10^{-6}. Therefore, we can conclude that this prediction cannot describe the very slow creation of leak paths. Hence, two assumptions can be made:

i. every leak paths are not detected, because cracks do not open – which is not very likely due to thermo-mechanical residual stresses, or because some cracks occur without delamination and does not connect to the network – which would contradict observations under loading, or because leak paths are too small to be detected, which does not seem to be the case, all identified leak paths being clearly identified with the leak detector;

ii. every ply are damaged but cracks of adjacent plies do not intersect. The infinite crack length hypothesis would therefore lead to an overestimation of the leak path number. Assuming crack length is finite, and depending on spatial organisation of cracks, a high crack rate may lead to a few intersections.

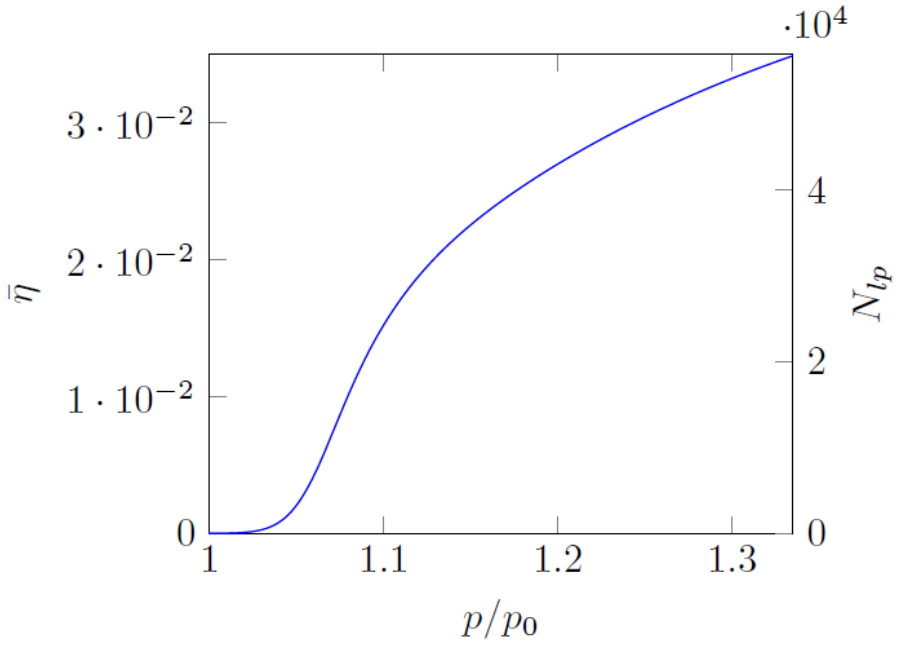

Figure 9: Leak path density $\bar{\eta}$ and leak path number N_{lp} vs. internal pressure (pressure adimensioned with respect to first-leak-path pressure).

Second hypothesis is the most likely. However, further observations have to be performed since references addressing crack distribution and length and interactions between plies are rare and contradictory [10,11].

5 CONCLUSIONS

Permeability experiments with leak path number assessment have been conducted. Analysis of the results reveals a slow leak path creation phase. A progressive damage evolution law was proposed, identified and applied to leak path prediction. Numerical results do not agree with the experiments, which is suggestive of the importance of further studying spatial organisation of cracks. Future research might focus on the choice of relevant geometric assumptions on the leakage network in order to improve the leak path density prediction.

ACKNOWLEDGEMENTS

The authors wish to thank the CNES and Region Aquitaine for their support.

REFERENCES

[1] C. Bois, J.-C. Malenfant, J.-C. Wahl, and M. Danis, A multiscale damage and crack opening model for the prediction of flow path in laminated composite. *Composites Science and Technology* 97, pp. 81–89, 2014.

[2] H. Darcy, *Les fontaines publiques de la ville de Dijon*. 1856.

[3] Y. Jannot and D. Lasseux, A new quasi-steady method to measure gas permeability of weakly permeable porous media. *Review of Scientific Instruments* 83, 2012, pp. 015113.

[4] C. Huchette, Sur la complémentarité des approches expérimentales et numériques pour la modélisation des mécanismes d'endommagement des composites stratifiés. *PhD thesis. France: Paris 6 University*, 2005.

[5] C. Huchette, D. Lévêque, and N. Carrère, A multiscale damage model for composite laminate based on numerical and experimental complementary tests. *In: Proceedings of the IUTAM Symposium on Multiscale Modelling of Damage and Fracture Processes in Composite Materials*, Dolny. 2006.

[6] P. Ladevèze and G. Lubineau, Relationships between 'micro' and 'meso' mechanics of laminated composites. *Compte Rendu Mécanique*, vol. 331, no. 8, pp. 537–544, 2003.

[7] D. Leguillon, Strength or toughness? A criterion for crack onset at a notch. *Eur J Mech A Solids* 21, pp. 61–72, 2002.

[8] P. Gudmundson and J. Alpman, Initiation and growth criteria for transverse matrix cracks in composite laminates. *Composites Science and Technology* 60, pp. 185–195, 2000.

[9] A. Parvizi, K.W. Garrett, and J.E. Bailey, Constrained cracking in glass fibre-reinforced epoxy cross-ply laminates. *J Mater Sci* 13, pp. 195–201, 1978.

[10] T. Yokozeki, T. Aoki, and T. Ishikawa, Consecutive matrix cracking in contiguous plies of composite laminates. *International Journal of Solids and Structures* 42, pp. 2785–2802, 2005.

[11] D.M. Grogan, S.B. Leen, C.O.A. Semprimoschnig, and CM Ó. Brádaigh, Damage characterisation of cryogenically cycled carbon fibre/PEEK laminates. *Composites Part A: Applied Science and Manufacturing* 66, pp. 237–250, 2014.